

Finite Element Simulation of the Temperature Cycling Tests

Cemal Basaran and Rumpa Chandaroy

Abstract—Temperature cycling tests are commonly used in the semiconductor industry to determine the number of cycles to failure and to predict reliability of the solder joints in the surface mount technology packages. In this paper, the thermomechanical fatigue of Pb40/Sn60 solder joint in a leadless ceramic chip carrier package is studied and [16] temperature cycling test is simulated by using a finite element procedure with the disturbed state concept (DSC) constitutive models. The progress of disturbance (damage) and the energy dissipated in the solder joint during thermal cycling are predicted. It is shown that the disturbance criterion used follows a similar path as the energy dissipation in the system. Moreover, the comparisons between the test data and the finite element analysis show that a finite element procedure using the DSC material models can be instrumental in reliability analysis and to predict the number of cycles to failure of a solder joint. Furthermore, the analysis gives a good picture of the progress of the failure mechanism and the disturbance in the solder joint.

Index Terms—Damage mechanics, electronic packaging, finite element analysis, solder joint.

I. INTRODUCTION

RELIABILITY of solder joints in surface mount technology (SMT) microelectronics packaging is a great concern to packaging design engineers. During its design life, the solder joint in SMT package experiences a wide range of temperature variations, which may vary between -40°C and 150°C , or may even be wider in automotive applications. Although a variety of mechanisms (e.g. vibration, corrosion, diffusion, mechanical shock, etc.) may lead to solder joint failure, the primary mechanisms are thermal stress and low-cycle strain-controlled fatigue, [23]. Fatigue failure of materials and structures is due to the initiation and propagation of fatigue fractures under the action of the repeated removal and reversal of the applied load. If this load is produced by thermally induced stresses than thermal fatigue occurs, [40]. Fatigue damage is usually the result of stress concentrations caused by dislocation pileups due to inelastic to-and-fro slipmotion of lattice defects and due to sliding between grains at the boundaries. The dislocation slip motion is caused by mechanical stresses, [8].

The connected components have different coefficients of thermal expansion (CTE) and different material properties. Because of the CTE mismatch, different elongation and contractions take place in the components. These components

Manuscript received January 1996; revised October 28, 1996. This work was sponsored by the Department of Defense Office of Naval Research Young Investigator Award program.

The authors are with the Department of Civil, Structural, and Environmental Engineering, State University of New York, Buffalo, NY 14260 USA.

Publisher Item Identifier S 1070-9886(97)09198-1.

experience relative motions during which shear and bending stresses are induced on the solder joint assembly. As a result of the temperature cycles, the solder joint experiences elastic, plastic and viscoplastic (time dependent, creep or relaxation) deformations. Eventually these deformations cause the accumulation of microcracking and damage in the solder joint. When the damage energy exceeds the crack initiation energy of the material, the initiation of cracks becomes inevitable.

Thermal cycling is an accepted experimental procedure for conducting surface mount technology package solder joint reliability testing under accelerated conditions, [6]. These experiments are very commonly used in the microelectronics industry. The only information these tests provide is the number of temperature cycles that are needed to fail a solder joint. The failure of the solder joint does not, however, give any information concerning what and where the problem is or where the damage initiated in the solder joint. Furthermore, the results of these experiments do not provide information on the stress distribution and microcracking zones in the joint. Hence these tests are limited in their usefulness to understand the thermomechanical damage behavior of the solder joint. There is, therefore, a need for a numerical analysis procedure, such as finite element method, which contains a unified constitutive models for materials in order to supplement the temperature cycling tests. This nonlinear numerical analysis procedure would be instrumental in studying the thermomechanical damage mechanics of solder joints.

A number of researchers have proposed constitutive models to study damage mechanics of solder alloys. Some of them are [1], [6]–[8], [14], [15], [19], [20], [22], [24], [26], [28], [30], [32]–[34], [36], [38], [39], [41], [42], [46], and others. “A common shortfall of these models is that most are empirical in nature and do not include the microstructural behavior that occurs in Sn/Pb solder during thermomechanical fatigue,” Frear *et al.* [14]. It should be pointed out that most of the proposed constitutive models in the literature are verified by backpredicting the same test data that was used to obtain the material parameters. This latter approach of curve fitting is not a good method to prove that the proposed model is a robust constitutive model based on the rules of the theory of plasticity [11]. Moreover, backpredicting the test data that was used to obtain the material constants usually yields an excellent match but when a different stress path or just a different test is backpredicted the results are usually less than satisfactory.

II. THE DISTURBED STATE CONCEPT (DSC)

The idea for this theory was originally proposed by Desai [1974] in order to characterize the behavior of the over

consolidated clays. The Disturbed State Concept is a unified modeling theory for the characterization of the mechanical behavior of materials and interfaces. This theory allows for the incorporation of the internal microstructural changes and the resulting micromechanisms in a deforming material into the macro-level constitutive model. When a material is subjected to external excitation, the material is initially in the relative intact state. As the disturbances increase the material transforms from the intact state to the fully adjusted (critical) state. Henceforth, at any given time the material is composed of randomly distributed clusters of the material in the relative intact and in the fully adjusted states. Consequently, the observed response of the material is defined by a combination of the response of the intact part and the response of the fully adjusted part of the material.

According to the DSC due to discontinuities within the material, it cannot be treated as though it were a continuum. Therefore, the discontinuum nature of the material should be taken into consideration in the constitutive model. Furthermore, the material model should also take into account the relative strain and the material moment that take effect when the material is disturbed. A detailed explanation of the DSC is given in [2], [5], and [12].

DSC is particularly well suited to characterize thermomechanical behavior of Pb/Sn solder alloys, because of the fact that Pb/Sn is a two-phase material containing Pb-rich and Sn-rich phases, [4]. Lead-rich phase region has been observed to correlate strongly with strain localization, [damage] and subsequent failure, and moreover Lead-rich and Tin-rich phases have different stress-strain responses, [14]. Therefore, having the capability to define a material with two distinct phases makes DSC more effective to characterize the behavior of materials with two phases, compared to other continuum mechanics models where the material is considered as one phase only.

According to the DSC, the equilibrium at a point is given by

$$d\sigma_{ij}^a = (1 - D)d\sigma_{ij}^i + D d\sigma_{ij}^c + dD(\sigma_{ij}^c - \sigma_{ij}^i) \quad (1)$$

where dD and D are the increment of damage and the damage, respectively. $d\sigma_{ij}^a$ is the observed incremental stress tensor, $d\sigma_{ij}^i$ and σ_{ij}^i are the increment of stress tensor and total stress tensor for the intact part, respectively. $d\sigma_{ij}^c$ and σ_{ij}^c are the increment of stress tensor and total stress tensor for the fully adjusted part, respectively.

The damage in the material can be expressed in terms of internal variables such as the trajectory of the inelastic strains, density, wave velocity, number of cycles experienced, entropy and energy dissipated. The progress of the disturbance in the material may be represented by using different functions: Weibull type exponential function from statistical theory of strength, [21], or a function of the energy dissipated in the system [5], [8] or a function of the disorder (entropy) of the system from statistical mechanics and thermodynamics, [25]. In this study, the following function is used for the progress of damage, D

$$D = u(1 - e^{-A\xi_D^Z}) \quad (2)$$

where A and Z are material constants and ξ_D is the trajectory of inelastic strain given by

$$\xi_D = \int \sqrt{dc_{ij}^p dc_{ij}^p} \quad (3)$$

where dc_{ij}^p is the incremental deviatoric inelastic strain tensor.

Implementing the thermo elasto-viscoplastic DSC material model in the equilibrium equation (1) yields the following constitutive relationship, [2]

$$d\sigma_{ij}^a = {}^{\text{DSC}}C_{ijkl}^{\text{ep}} d\varepsilon_{kl}^i \quad (4)$$

where $d\varepsilon_{kl}^i$ is the incremental total strain tensor for the intact part and the DSC constitutive tensor is given by

$${}^{\text{DSC}}C_{ijkl}^{\text{ep}} = [(1 - D){}^iC_{ijkl}^{\text{ep}} + D(1 + \alpha){}^cC_{ijkl}^{\text{ep}} + (\sigma_{ij}^c - \sigma_{ij}^i)R_{kl}] \quad (5)$$

where ${}^iC_{ijkl}^{\text{ep}}$ and ${}^cC_{ijkl}^{\text{ep}}$ are the tangential elasto-[visco]plastic constitutive tensor for the intact part and the fully adjusted part, respectively. α is an empirical coefficient of relative motion between the intact part and fully adjusted part and R_{kl} is given by

$$R_{st} = \frac{[D_u A Z \xi_D^{Z-1} e^{-A\xi_D^Z}] \frac{\partial F}{\partial \sigma_{uv}} C_{uvst}^e \left(\frac{\partial F}{\partial \sigma_{ij}} \frac{\partial F}{\partial \sigma_{ij}} - \frac{1}{3} \frac{\partial F}{\partial \sigma_{ii}} \frac{\partial F}{\partial \sigma_{ii}} \right)^{\frac{1}{2}}}{\left[\frac{\partial F}{\partial \sigma_{mn}} C_{mnpq}^e \frac{\partial F}{\partial \sigma_{pq}} - \frac{\partial F}{\partial \xi} \left(\frac{\partial F}{\partial \sigma_{mn}} \frac{\partial F}{\partial \sigma_{mn}} \right)^{\frac{1}{2}} \right]} \quad (6)$$

where F is the yield surface given by

$$F = \frac{J_{2D}}{P_a^2} - \left[\left(\frac{J_1(\theta)}{P_a} \right)^2 (\gamma(\theta) - \bar{\alpha}(\theta)) \right] \quad (7)$$

where J_1 is the first invariant of the stress tensor, J_{2D} is the second invariant of the deviatoric stress tensor. P_a is the atmospheric pressure, θ is the temperature, $\gamma(\theta)$ is the temperature dependent ultimate stress state material constant and $\bar{\alpha} = \frac{a_1(\theta)}{\xi^{\eta_1(\theta)}}$ is the hardening function with $a_1(q)$, $\eta_1(\theta)$ temperature dependent material constants. The procedure for obtaining these material constants from experimental data is given in [5]. It should be pointed out that all the material parameters in DSC models have physical meanings and each parameter represents certain characteristics of the material.

If we study (5) we realize that if the disturbance, D , is not included the DSC constitutive model would be reduced to the continuum formulation. If we ignore the stresses and the strain in the fully adjusted part, the formulation reduces to Kachanov [1986] continuum damage model. The DSC formulation also allows for the relative motions between the intact and fully adjusted parts. Furthermore, DSC also allows for the inclusion of the internal moment in the material, because the stresses in the two parts are different. The term R_{kl} may be treated as an implicit moment arm for the internal moment.

III. VERIFICATION OF THE CONSTITUTIVE MODEL

In order to verify the constitutive model experimental data reported in the literature is back predicted. The test data used here for verification was not used to obtain the material constants.

The test data used is the isothermal uniaxial extension experiment results reported by Guo *et al.* [15]. The authors studied

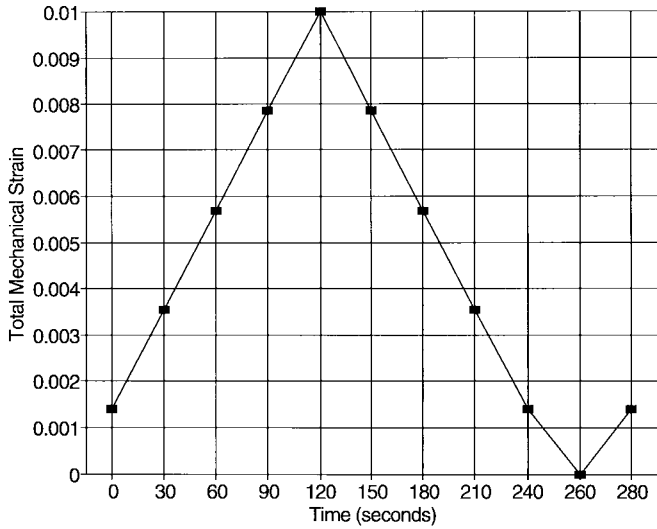


Fig. 1. Applied total mechanical strain versus time history.

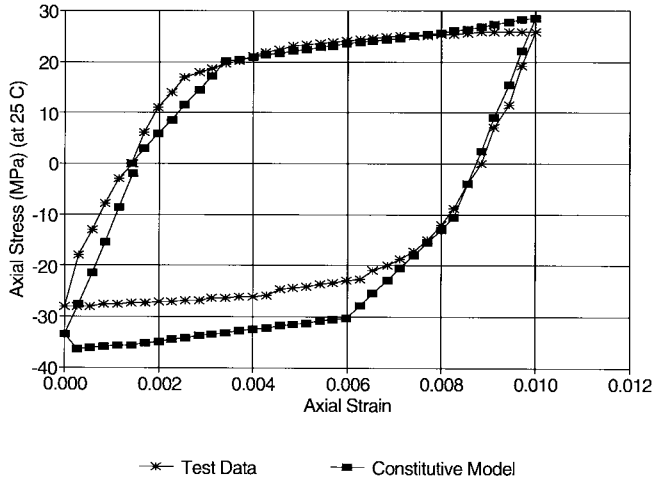


Fig. 2. Model predictions versus isothermal (25 °C) uniaxial tension test data [15].

the isothermal (25 °C) fatigue of a Pb36.37/Sn63.2/Sb0.31 solder under total strain-controlled tests. The specimen dimensions were 12 mm × 12 mm × 6.4 mm in gauge section. The isothermal fatigue testing was performed under uniaxial total strain control with the total strain range up to one percent., Fig. 1. Pb40/Sn60 material properties were used in the finite element analysis. Because the test was conducted as a strain-controlled experiment, in the finite element analysis displacements were prescribed. Fig. 2 shows comparison of isothermal (25 °C) test data versus the finite element predictions for the average axial stress versus the axial strain. The results show that the isothermal uniaxial tension behavior of the material is predicted well. Small differences at the extreme points could be attributed to the fact that the material tested is Pb36.37/Sn63.2/Sb0.31 but the material properties used are for Pb40/Sn60.

IV. IMPLEMENTATION IN THE FINITE ELEMENT PROCEDURE

Implementing the above constitutive equations in the displacement based finite element method yields the following

equilibrium equation [2]:

$$\begin{aligned} & \int_V [B]^T [r^{-1} L_n^{\text{ep}\theta}] [B] dV \{d^r q_{n+1}\} \\ & = \{Q_{n+1}\} - \int_V [B]^T \{r^{-1} \sigma_n^a\} dV \\ & \quad - \int_V [B]^T \{r^{-1} \sigma_n^c - r^{-1} \sigma_n^i\} dD_n dV \\ & \quad + \int_V \Delta t_n [B]^T [r^{-1} L_n^{\text{ep}\theta}] \{r^{-1} \dot{\epsilon}_n^{\text{vp}\theta}\} dV \\ & \quad + \int_V \Delta t_n \chi d\theta_n [B]^T [r L_n^{\text{ep}\theta}] [r^{-1} G_2]_n \{\bar{T}\} dV \\ & \quad + \int_V \alpha_T d\theta [B]^T [r L_n^{\text{ep}\theta}] dV \end{aligned} \quad (8)$$

where n is the load/temperature increment number and r is the iteration number, the effective constitutive matrix is given by

$$[{}^r L_n^{\text{ep}\theta}] = (1 - D_n) [{}^i C_n^{\text{ep}\theta}] + D_n (1 + \alpha_n) [{}^c C_n^{\text{ep}\theta}] \quad (9)$$

$[B]$ is the strain-displacement transformation matrix, V is the volume, $\{dq\}$ is displacement increment vector, $\{Q\}$ nodal force vector, Δt is the time step increment, χ is the time integration scheme coefficient, $d\theta$ is the increment of temperature, α_T is the coefficient of thermal expansion and $[G_2]_n = [\frac{\partial \dot{\epsilon}^{\text{vp}\theta}}{\partial \theta}]_n$ and the viscoplastic strain rate is given by [28]

$$\{\dot{\epsilon}^{\text{vp}\theta}\} = A (\sinh B \{\sigma\})^n (d)^m \exp(-Q/RT) \quad (10)$$

where A ($2.9524E+8$) and B (0.125938) are material constants $\{\sigma\}$ is the stress vector, d is the average grain size ($28.4 \mu\text{m}$), Q is the apparent activation energy (61417 joule/mole), R is the gas constant (8.314 joule/mole), T is the absolute temperature, n is the stress exponent (1.88882) and m is the solder grain size exponent (-3.011).

V. ANALYSIS OF A LEADLESS CERAMIC CHIP CARRIER PACKAGE

Hall [1984] tested an 84 I/O, 0.64 mm pitch leadless ceramic chip carrier which is mounted on a printed wiring board (FR4, polyimide epoxy glass) by a Pb40/Sn60 eutectic solder joint. Solder joints in surface mount technology packages experience thermomechanical cycling in operating conditions. It is desirable to determine the number of cycles required to fail a solder joint. A few hundred cycles of -40 °C to $+130$ °C is typically enough to cause cracks and electrical failures [35]. Surface mount technology provides greater space for interconnections, but is susceptible to thermal fatigue due to a coefficient of thermal expansion mismatch between the joined layers.

The package was subjected to temperature cycling between 25 °C and 125 °C. The temperature cycle versus time change used in this study is given in Fig. 3, with the exception of 2 hr hold time at -25 °C. The finite element discretization of the package is shown in Fig. 4. Because of the symmetry of the structure, only one-half of the system is shown. In the finite element analysis leadless ceramic chip carrier and the printed wiring board are modeled as elastic materials with plane strain idealization and the solder joint is modeled with axisymmetric idealization. The intact part of the solder joint

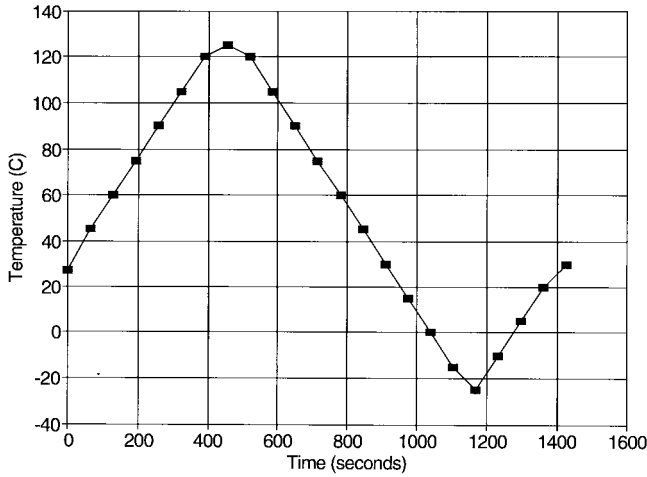


Fig. 3. Time history of the temperature cycle, [2 h hold time at 25 °C not shown].

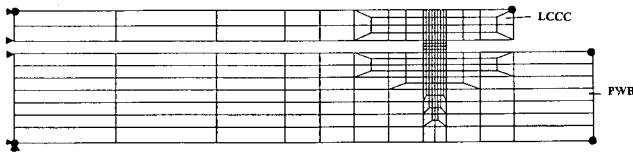


Fig. 4. Finite element mesh used for analysis.

is modeled with thermo elasto-viscoplastic with disturbance material model. The fully adjusted part is assumed to carry no shear stresses but hydrostatic stresses only. The following material parameters are used in the following analysis.

Elastic modulus $E = 15.2-65.5 T(^{\circ}\text{C})$ GPa, [6] Poisson's ratio $\nu = 0.4(\frac{\theta}{300})^{0.14}$, ultimate state parameter $\gamma = 0.00082(\frac{\theta}{300})^{-0.034}$, hardening parameters $a_1 = 0.000024(\frac{\theta}{300})^{-2.578}$ and $\eta_1 = 0.394$, coefficient of thermal expansion $\alpha_T = 3.0(\frac{\theta}{300})^{0.24}10^{-6}$, fluidity parameter $\Gamma = 1.8(\frac{\theta}{300})^{6.185}/\text{sec}$ and flow function exponent $N = 2.67$. Disturbance parameters $Z = 0.676$ and $A = 0.102(\frac{\theta}{300})^{1.55}$. These material parameters are obtained from experimental data in the literature such as, uniaxial tension data by [31], cyclic isothermal simple shear data by [37], creep data reported by [28], and uniaxial tension and creep data by [36]. It should be emphasized that the material constants were obtained from different tests not from the test data that is being backpredicted in here. It is very common in the literature to obtain material constants from a test data and then to back predict the same data. The latter procedure yields very good match between the test data and the prediction, however, it does not prove that the constitutive model would characterize the material behavior for all stress paths.

In the finite element analysis variable time step scheme is used and initial time increment is 0.00001 s. The time step criteria given by [27],

$$\Delta t_{n+1} \leq \tau \frac{\epsilon_n}{d\epsilon_n^{\text{vp}}} \quad \text{and} \quad \Delta t_{n+1} \leq 1.5\Delta t_n \quad (11)$$

where τ is a coefficient, ϵ_n is the total strain, and $d\epsilon_n^{\text{vp}}$ is the viscoplastic strain increment. For the time increment

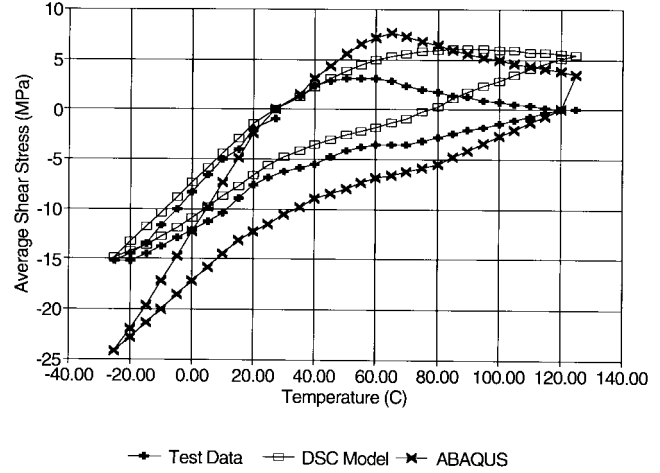


Fig. 5. DSC based FEM results versus test data and ABAQUS results [29].

parameter, τ , value in the hardening range 0.1 to 0.15 and near collapse 0.01 to 0.005 were found necessary, [45].

VI. DISCUSSION OF THE RESULTS

The comparison of the finite element results versus the test data for the first temperature cycle is given in Fig. 5. The test data for the subsequent cycles is not available in the literature therefore comparison is presented for the first cycle only. Fig. 5 also shows results reported by [29] for the same problem. Pao *et al.* [29] results are obtained by implementing a modified version of Knecht and Fox [22] model in ABAQUS finite element computer program. The shear stress shown in the figure is the average shear stress calculated at the middle of the solder joint, i.e. at the one half height. The results show a good correlation between the experimental results and the DSC predictions. The main difference is that the finite element with DSC material models results show 5MPa shear stress in the solder joint at 125 °C. There are a number of reasons for this deviation: One of them is that at this temperature, the solder is almost liquid with zero shear strength according to the test results, however the function used to characterize the elastic modulus yields a shear modulus of 2.4 GPa. Using a zero shear strength in the finite element formulation is not numerically possible. Another problem is that these Hall [16] experimental results are not used to determine the material parameters. Some of the experiment results reported by Riemer [31], which are used in this study to determine the material parameters, at 125 °C, show that the material does carry shear at that temperature. The qualitative trend in this finite element prediction is similar to the test results.

Fig. 6 shows the response of the solder in the temperature cycles upto 250th cycle. Fig. 7 depicts the average disturbance progress in the solder joint versus the number of cycles. Average disturbance in the solder joint is obtained by adding up disturbance, D , values at all Gauss points and dividing the sum by the number of the total Gauss points in the mesh. Hall and Sherry [17] and Pan [28] report that the solder joint failed at 346th temperature cycle. If we study Fig. 7 we realize that the disturbance experiences a sharp turn around 350 cycles. This result is in compliance with the experiments.

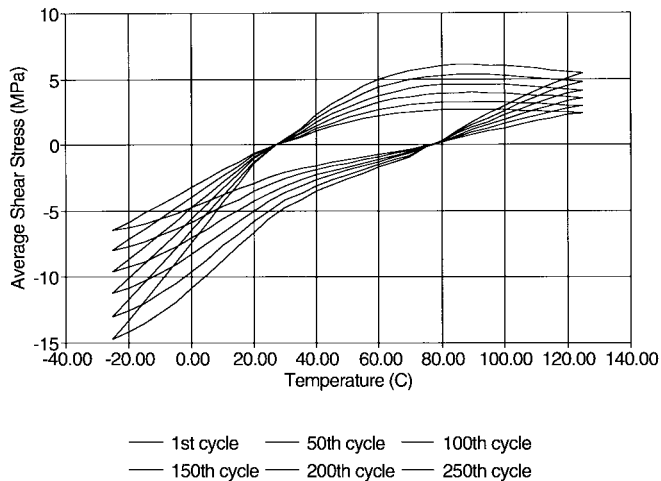


Fig. 6. DSC based FEM results for temperature cycles 1, 50, 100, 150, 200, 250.

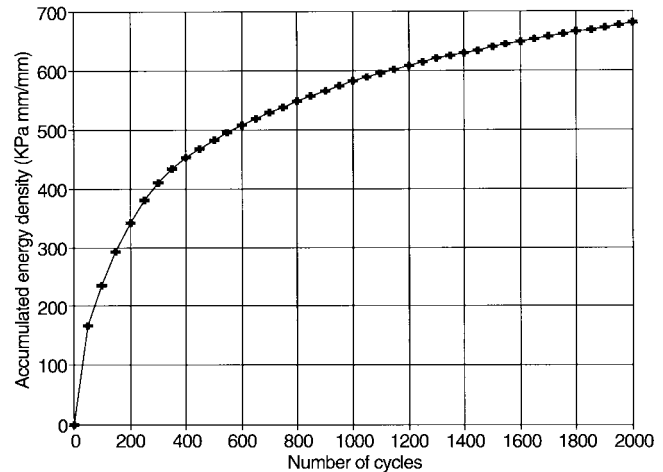


Fig. 8. Accumulated energy density in the solder joint versus the number of temperature cycles.

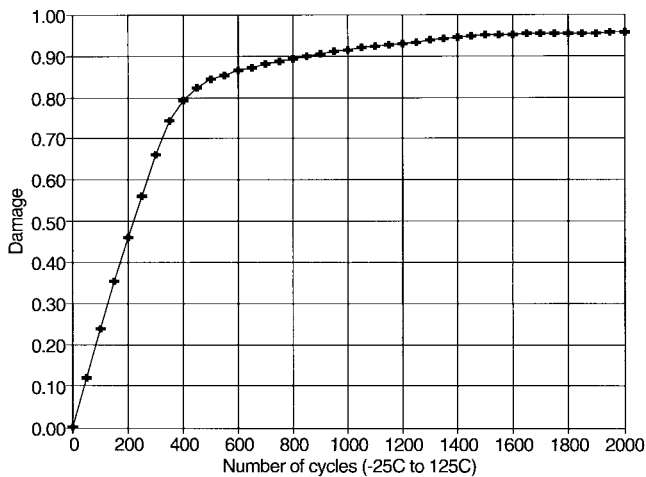


Fig. 7. Average damage in the solder joint versus the number of temperature cycles.

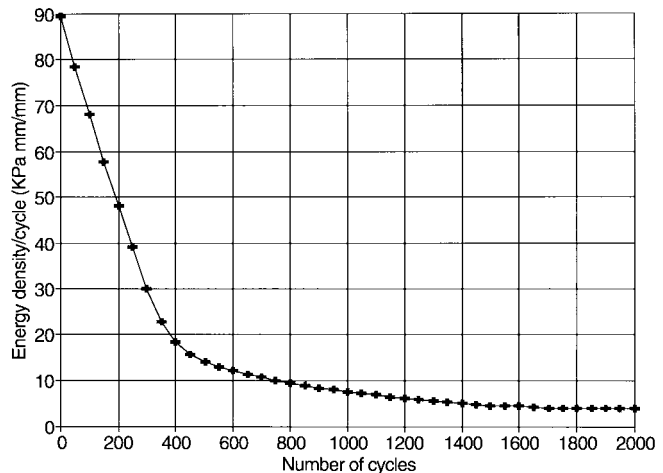


Fig. 9. Energy density in the solder joint versus the number of temperature cycles.

Fig. 8 shows the accumulated energy density of the solder joint. Accumulated energy density of the solder joint is obtained by simple summation of the energy density per cycle. Accumulated energy density increases almost linearly up to 350 cycles, after which it starts to increase at a decreasing rate. If we study the curve we notice that the solder accumulates more energy in the first 350 cycles than the next 1650 cycles. Accumulated energy density in the first 350 cycles is about 450 KPa mm/mm and in the next 1650 cycles it is about 330 KPa mm/mm.

Fig. 9 depicts the energy density at the solder joint versus the number of temperature cycles. The DSC model predicts a sharp turn at 350th cycle. Fig. 10 shows the disturbance, D , distribution in the solder joint at the end of the first temperature cycle. If we study the figures we see that the upper right corner is the point at which the concentration of D initiates indicating microcracking, localization and crack propagation. This result is consistent with the crack propagation sequence reported by [17] and [28] for a similar solder joint. Eventually, the disturbance propagates along the upper side of the solder and

it reaches the maximum value, on that side while the bottom side experiences relatively lower disturbance. After about 350 temperature cycles almost all solder joint elements along the ceramic interface has the value of $D \geq 0.9$. Thus, if $D = 0.9$ is assumed to be the critical value, after which the complete upper side has cracked, then the solder joint can be considered to have failed. This result is consistent with the laboratory observed value of cycles to failure which is equal to about 346. Furthermore, the results of the analysis indicate that the zone with $D \geq 0.9$ only increases slightly, thereby shows that a relatively stable energy dissipation has been reached after the failure.

The elastic modulus used in this study is taken from [6] and [18]. There is a wide range spectrum of values reported for the Pb40/Sn60 solder alloy room temperature elastic modulus. Knecht and Fox [22] show that considerable variations exist in the published values of the elastic moduli of Pb40/Sn60 solder. For example, the quotes 12.4 GPa, 14.8 GPa, 30.0 GPa, and 43.4 GPa have been reported for the room temperature (27 °C) elastic modulus of Pb40/Sn60 solder alloy. The finite element analysis requires accurate material properties as input

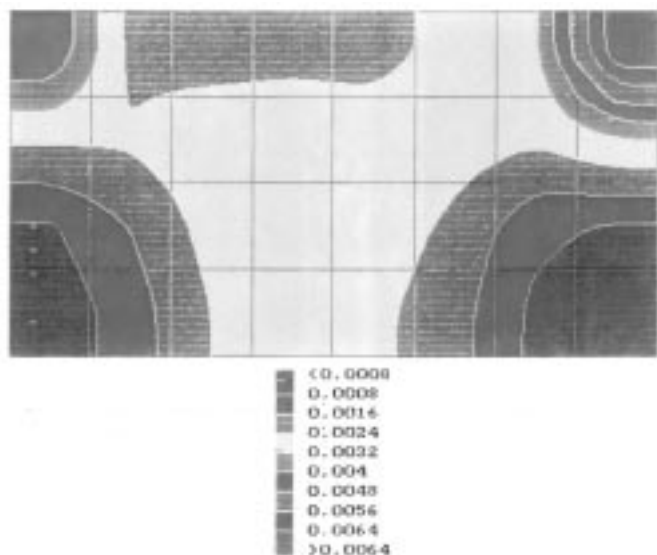


Fig. 10. Damage distribution in the solder joint at the end of the first thermal cycle.

as well as dimensions of the joint and the loading history. But, the finite element analysis results are particularly sensitive to the elastic modulus value. The finite element method is a numerical analysis procedure for solving partial differential equations. The solution converges to the exact solution of the partial differential equation as the discretization is refined for the strain hardening region of the stress-strain diagram. In the strain-softening region it is well known that finite element method experiences mesh sensitivity. In DSC models mesh sensitivity is dealt with nonlocal continuum based DSC average strain method, where the strain is averaged over a characteristic length. It has been demonstrated by many researchers, such as [3], [10], [45] that FEM can successfully be used to solve boundary value problems if accurate material constants and proper constitutive models are used.

It is well known that an exact analysis with strict adherence to the constitutive relations of linear elasticity yields a singularity at the intersection of the free edge with an interface of two dissimilar materials, [43]. When the material model is inelastic singularity does not occur because of the condition of consistency of the theory of plasticity, [11]. The condition of consistency requires that when the state of stress is outside the yield surface, as in the case of a singularity, it must be brought back to the yield surface with a return strategy. Further discussion on this subject is given in [2].

Another problem faced in obtaining the material constants is that most of the testing is performed on bulk solder. The size of bulk sample is large relative to the solder joint, Hall and Sherry [17] report that "The specimen size versus the microstructure size ratio effects may be important," in determining the mechanical behavior. Bonda and Noyan [4] have shown that the material properties of a microscale joint in an actual semiconductor device is different than the large bulk specimen of the solder alloy.

It should be emphasized that the results obtained here are strictly valid for the solder configuration used in this study.

Solder joint dimensions, height in particular, and the solder material affect the reliability and the thermal fatigue life. Discussion of this topic is outside the scope of this paper.

VII. CONCLUSION

In this paper a finite element procedure based on the Disturbed State Concept material models is proposed for the thermomechanical reliability analysis of solder joints in surface mount technology packaging. It has been shown that the thermomechanical behavior of microelectronics packaging solder joints can be predicted by proper constitutive models. Using the finite element procedure proposed herein, accelerated thermal cycling tests can be simulated and the proposed numerical procedure can be used in conjunction with the tests.

The Disturbed State Concept allows characterization of the material behavior to be represented in terms of two reference states of the material, namely the relative intact and the fully adjusted states. This feature makes DSC particularly powerful to characterize behavior of two phase materials, such as Pb/Sn alloys. Furthermore, the Disturbed State Concept allows us to have different stresses and strains in both the intact part and the fully adjusted parts of the material. Because of the differential strain in the material, we are able to account for the relative motions in the material. Considering the relative motion within the material provides us with a more accurate characterization of the energy of the material than the conventional continuum damage mechanics models do.

The results of this research can be instrumental in making predictions of reliability of interconnections under thermal cycling stresses. Material properties used in this study are obtained from experimental results published in the literature. The experiments backpredicted were not used to obtain material constants. Most of the time, a complete description of the test setup and conditions in which the tests were run are not available. Therefore, when the material constants are obtained, certain assumptions are made. The accurate determination of the material constants is crucial to the analysis since the finite element results are sensitive to the material parameters.

ACKNOWLEDGMENT

The authors would like to thank C. S. Desai, T. Kundu, and J. Prince, University of Arizona, Tucson, for their help.

REFERENCES

- [1] D. Barker, Vodzak, A. Dasgupta, and M. Pecht, "Combined vibrational and thermal solder joint fatigue—A generalized strain versus life approach," *J. Electron. Packag.*, vol. 112, pp. 129–134, 1990.
- [2] C. Basaran and C. S. Desai, *Finite Element Thermomechanical Analysis of Electronic Packaging Problems Using the Disturbed State Constitutive Models*, Report to NSF, Dept. Civil Engineering and Engineering Mechanics, Univ. of Arizona, Tucson, 1994.
- [3] K. J. Bathe, *Finite Element Procedures*. Englewood Cliffs, NJ: Prentice-Hall, 1996.
- [4] N. R. Bonda and I. C. Noyan, "Effect of specimen size in predicting the mechanical properties of Pb/Sn solder alloys," *IEEE Trans. Comp., Packag., Manufact. Technol.*, vol. 19, 1996.
- [5] J. Chia and C. S. Desai, *Constitutive Modeling of Thermomechanical Response of Materials in Semiconductor Devices With Emphasis on Interface Behavior*, Report to NSF, Depart. Civil Engineering and Engineering Mechanics, University of Arizona, 1994.

- [6] J.-P. Clech and J. A. Augis, "Engineering analysis of thermal cycling accelerated test for surface-mount attachment reliability evaluation," in *Proc. VII Ann. Electron. Packag. Conf.*, Boston, MA, Nov. 1987, vol. 1, pp. 385–411.
- [7] R. Darveaux, Y. Edward, I. Turlik, and K. I. Murty, "Mechanical characteristics of IN and Pb55Sn solders in a thinfilm multichip package," in *Proc. Mater. Res. Symp.*, vol. 203, pp. 443–449, 1991.
- [8] A. Dasgupta, C. Oyan, D. Barker, and M. Pecht, "Solder creep-fatigue analysis by an energy-partitioning approach," *Trans. ASME, J. Electron. Packag.*, vol. 114, 1992.
- [9] C. S. Desai, "A consistent finite element technique for work-softening behavior," in *Proc. Int. Conf. Comp. Meth. Nonlinear Mech.*, J. T. Oden et al., Eds. Austin, TX: Univ. of Texas Press, 1974.
- [10] ———, *Elementary Finite Element Method*. Englewood Cliffs, NJ: Prentice-Hall, 1979.
- [11] C. S. Desai and H. Siriwardane, *Constitutive Laws for Engineering Materials: With Emphasis on Geologic Materials*. Englewood Cliffs, NJ: Prentice-Hall, 1984.
- [12] C. S. Desai, "Constitutive modeling using the disturbed state as microstructure self-adjustment concept," in *Continuum Models for Materials with Microstructure*, H. B. Muhlhaus, Ed. New York: Wiley, 1996.
- [13] C. S. Desai, C. Basaran, and Z. Wu, "Numerical algorithms and mesh sensitivity in disturbed state concept models," *Int. J. Numer. Meth.*, vol. 40, pp. 3059–3083, 1997.
- [14] D. R. Frear, S. N. Burchett, and M. M. Rashid, "A microstructurally based model of solder under conditions of thermomechanical fatigue," *Trans. ASME Adv. Electron. Packag.*, vol. EEP-10, no. 1, 1995.
- [15] Q. Guo, E. C. Cutiongco, L. M. Keer, and M. E. Fine, "Thermomechanical fatigue life prediction of 63Sn/37Pb solder," *Trans. ASME, J. Electron. Packag.*, vol. 114, pp. 145–151, June 1992.
- [16] P. Hall, "Forces, moments and displacements during thermal chamber cycling of leadless ceramic chip carriers soldered to printed boards," *IEEE Trans. Comp., Hybrids, Manufact. Technol.*, vol. CHMT-7, pp. 314–327, 1984.
- [17] P. M. Hall and W. M. Sherry, "Materials, structures, and mechanics of solder-joints for surface-mount microelectronics technology," in *Proc. Lectures 3rd Int. Conf. Techniques de Connexion en Electronique*, Welding Society, Fellbach, Dusseldorf, Germany, Feb. 1986, pp. 18–20.
- [18] C. A. Harper, *Handbook of Materials and Processes for Electronics*. New York: McGraw-Hill, 1970.
- [19] J. H. Huang, J. Y. Pei, Y. Y. Qian, and Y. H. Jiang, "Life predictions of SMT solder joints under thermal cycling," *Soldering Surface Mount Technol.*, 1994, vol. 16, pp. 31–50.
- [20] H. Ishikawa and K. Sasaki, "Constitutive model for 60Sn-40Pb solder under cycling loading," *Adv. Electron. Packag.*, in *Proc. Joint ASME/JSME Conf. Electron. Packag.*, W. T. Chen and H. Abe, Eds., 1992, vol. 1, pp. 401–408.
- [21] L. M. Kachanov, *Introduction of Continuum Damage Mechanics*. Amsterdam, The Netherlands: Martinus Nijhoff, 1986.
- [22] S. Knecht and L. R. Fox, "Constitutive relation and creep-fatigue life model for eutectic tin-lead solder," *IEEE Trans. Comp., Hybrids, Manufact. Technol.*, vol. 13, pp. 424–433, June 1990.
- [23] J. H. Lau, D. W. Rice, and D. A. Avery, "Elasto plastic analysis of surface mount solder joints," *IEEE Trans. Comp., Hybrids, Manufact. Technol.*, vol. CHMT-10, Sept. 1987.
- [24] J. Lau and S. Erasmus, "Reliability of fine pitch plastic quad flat pack leads and solder joints under bending twisting and thermal conditions," *J. Electron. Packag.*, vol. 115, pp. 322–328, 1993.
- [25] H. B. Muhlhaus, "A thermodynamic criteria for damage," in *Proc. 8th Int. Conf. Int. Assoc. Comput. Methods Adv. Geomech.*, WV, May 1994, pp. 22–28.
- [26] Y. Oshida and P. Chen, "High and low-cycle fatigue damage evaluation of multilayer thin film structure," *Trans. ASME, J. Electron. Packag.*, vol. 113, Mar. 1991.
- [27] D. R. J. Owen and E. Hinton, *Finite Elements in Plasticity*. Swansea, U.K.: Pineridge.
- [28] T. Pan, "Thermal cycling induced plastic deformation in solder joints: Part III: Strain-energy based fatigue life model and effects of ramp rate and hold time," in *Proc. ASME Winter Ann. Meet.*, Atlanta, GA, Dec. 1991, pp. 1–6.
- [29] Y. H. Pao, K. L. Chen, and A. Y. Kuo, "A nonlinear and time dependent finite element analysis of solder joints in surface mounted components under thermal cycling," in *Proc. Mat. Res. Soc. Symp.*, 1991, vol. 226.
- [30] Y. H. Pao, R. Govila, S. Badgley, and E. Jih, "An experimental and finite element study of thermal fatigue fracture of PbSn solder joints," *J. Electron. Packag.*, vol. 115, pp. 1–8, 1993.
- [31] E. D. Riemer, "Prediction of temperature cycling life for SMT solder joints on TCE-mismatched substrates," in *Proc. Electron. Comp.*, 1990, pp. 418–423.
- [32] R. G. Ross, L. C. Wen, G. R. Mon, and E. Jetter, "Solder creep-fatigue interactions with flexible leaded parts," *J. Electron. Packag.*, vol. 114, pp. 185–192, 1992.
- [33] J. Sauber and Seyyedi, "Predicting thermal fatigue lifetimes for SMT solder joints," *J. Electron. Packag.*, vol. 114, pp. 472–476, 1992.
- [34] C. G. Schmidt, "A simple model for fatigue of leadless ceramic chip carrier solder attachments," *J. Electron. Manufact.*, vol. 2, pp. 31–36, 1992.
- [35] W. M. Sherry, J. S. Erich, M. K. Bartschat, and F. B. Prinz, "Analytical and experimental analysis of LCCC solder joint fatigue life," in *Proc. Electron. Comp. Conf.*, 1985, pp. 81–90.
- [36] A. Skipor, S. Harren, and J. Botsis, "Constitutive characterization of 63/37 Sn/Pb eutectic solder using the bodner-partom unified creep-plasticity model," *ASME, Adv. Electron. Packag.*, pp. 661–672, 1992.
- [37] H. D. Solomon, "Low cycle fatigue of 60/40 solder plastic strain limited vs. displacement limited testing," *Electron. Packag.: Mater. Processes*, pp. 29–47, 1989.
- [38] H. D. Solomon and E. D. Tolksdorf, "Energy approach to the fatigue of 60/40 solder: Part II—Influence of hold time and asymmetric loading," *J. Electron. Packag.*, vol. 118, pp. 67–71, 1996.
- [39] R. Subrahmanyam, J. R. Wilcox, and C. Li, "A damage integral approach to thermal fatigue of solder joints," *IEEE Trans. Comp., Hybrids, Manufact. Technol.*, vol. 12, Dec. 1989.
- [40] E. Suhir, "Thermal stress failures in microelectronic components—review and extension," in *Advances in Thermal Modeling of Electronic Components and Systems*, A. Bar-Cohen and A. Kraus, Eds. 1989, ch. 5, vol. 1, pp. 337–412.
- [41] J. K. Tien, B. C. Hendrix, and A. I. Attarwala, "Understanding the cyclic mechanical behavior of lead/tin solder," *Trans. ASME, J. Electron. Packag.*, vol. 113, June 1991.
- [42] S. Verma, A. Dasgupta, and D. Barker, "A Numerical study of fatigue life of J-leaded solder joints using the energy partitioning approach," *J. Electron. Packag.*, vol. 115, pp. 416–423, 1993.
- [43] W. L. Yin, "Thermal stresses and free-edge effects in laminated beams: A variational approach using stress functions," *J. Electron. Packag.*, vol. 113, pp. 68–75, 1991.
- [44] O. C. Zienkiewicz, *The Finite Element Method*. New York: McGraw Hill, 1986.
- [45] O. C. Zienkiewicz and I. C. Comeau, "Viscoplasticity-plasticity and creep in elastic solids—a unified approach," *Int. J. Numer. Meth. Eng.*, vol. 8, pp. 821–845, 1974.
- [46] A. Zubelewicz, Q. Guo, E. C. Cutiongco, M. E. Fine, and L. M. Keer, "Micromechanical method to predict fatigue life of solder," *J. Electron. Packag.*, vol. 112, 1990.



Cemal Basaran received the M.S. degree from the Massachusetts Institute of Technology, Cambridge, and the Ph.D. degree from the University of Arizona, Tucson.

He is an Assistant Professor in the Department of Civil, Structural, and Environmental Engineering, State University of New York, Buffalo. His research interest is in experimental and computational reliability study of interconnects and interfaces in electronic packaging under combined dynamic and thermal loading.

Dr. Basaran received the DoD ONR Young Investigator Award for his research on damage mechanics of power electronic packaging interconnects and interfaces in 1997.



Rumpa Chandaroy received the M.S. degree from the State University of New York, Buffalo, and is currently pursuing the Ph.D. degree in thermomechanical response of solder joints under concurrent dynamic and thermal cycling loading at the Department of Civil, Structural, and Environmental Engineering.

Ms. Chandaroy received the India National Scholarship.